Free Space Ramsey Spectroscopy in Rubidium with Noise below the Quantum Projection Limit

Benjamin K. Malia[1], Julián Martínez-Rincón[1], Yunfan Wu[2], Onur Hosten[3], and Mark A. Kasevich[1,2,*]

[1]*Department of Physics, Stanford University, Stanford, California 94305, USA*
[2]*Department of Applied Physics, Stanford University, Stanford, California 94305, USA*
[3]*Institute of Science and Technology Austria, Klosterneuburg 3400, Austria*

We demonstrate the utility of optical cavity generated spin-squeezed states in free space atomic fountain clocks in ensembles of 390 000 ^{87}Rb atoms. Fluorescence imaging, correlated to an initial quantum nondemolition measurement, is used for population spectroscopy after the atoms are released from a confining lattice. For a free fall time of 4 milliseconds, we resolve a single-shot phase sensitivity of 814(61) microradians, which is 5.8(0.6) decibels (dB) below the quantum projection limit. We observe that this squeezing is preserved as the cloud expands to a roughly 200 μm radius and falls roughly 300 μm in free space. Ramsey spectroscopy with 240 000 atoms at a 3.6 ms Ramsey time results in a single-shot fractional frequency stability of $8.4(0.2) \times 10^{-12}$, 3.8(0.2) dB below the quantum projection limit. The sensitivity and stability are limited by the technical noise in the fluorescence detection protocol and the microwave system, respectively.

Quantum sensors are important for a variety of applications including time keeping and gravitational sensing [1–3]. An atomic fountain clock, for example, works by releasing a cloud of ultracold atoms into free space and exposing them to a reference microwave source. A relative phase accumulated due to differences between the microwave and atomic frequency reveals itself in a difference in population between two atomic states [4].

Measurements of these population differences in an ensemble of uncorrelated atoms are limited by the quantum projection noise (QPN). For a fixed atom number $N = N_1 + N_2$, the variance is such that $\text{var}(N_1 - N_2) = 4\text{var}(N_1) = 4\text{var}(N_2) \approx N$ if $N_1 \approx N_2 \approx N/2$ [5]. Surpassing the QPN using quantum correlated initial states of the atoms is an appealing path when increasing the total number of atoms or the interrogation time is technically limited.

Different approaches exist for preparing entangled states of large atomic ensembles, with spin squeezing—reducing the quantum statistical noise in one of the components of the collective pseudospin [5,6]—being the most successful to date [7,8]. Up to 20 dB in metrologically relevant variance reduction is obtained by performing quantum nondemolition (QND) measurements in cavity-QED systems with up to one million atoms [8–10]. These measurements probe the cavity resonance frequency that is modified by the dispersive atom-light interactions, with a sensitivity below the QPN, and reduce the variance of the atomic spin while preserving its mean.

Many approaches toward highly sensitive sensors rely on keeping the atoms confined to an optical lattice during the interrogation time [1]. When squeezing is desired for metrological enhancement in such scenarios, the atoms are prepared and probed using an optical cavity. Detection via absorption imaging is also possible with a trapped Bose-Einstein condensate (BEC) [11], and fluorescent imaging has been used to detect trapped ions [12].

For atomic clock performance [13], in particular, 10.5(3) dB metrological enhancement was recently shown for a Ramsey time of 228 μs using 100 000 atoms [9]. In-lattice configurations, however, do not allow for long falls in free space since the atoms must be recaptured, limiting their capabilities as inertial sensors. Their performance is degraded due to the spatial-dependent coupling of the expanded atom cloud to the cavity light mode [14]. These issues degrade the amount of metrologically relevant squeezing recovered and limit the performance of the sensor to short interrogation periods.

Fluorescence population spectroscopy is a good candidate to allow for much longer interrogation times and to discard the necessity of optical cavity and lattice operation after state preparation. While the state-preparation step is necessarily quantum nondestructive, the subsequent population spectroscopy only requires high fidelity atom counting, and can be destructive. Fluorescence imaging has been previously used for single atom counting resolution with ^{87}Rb [15] and was also demonstrated to detect spin-nematic quadrature squeezing in a spin-1 ^{87}Rb BEC system [16].

In this Letter, we report a method for incorporating cavity-generated spin squeezed states into free space atomic sensors. The method is able to resolve spin

squeezed states of 390 000 ^{87}Rb atoms with up to 5.8 dB in metrologically relevant variance reduction for a fluorescence collection time of 3 ms using a CMOS camera [17]. This squeezing level is resolved for all times as the cloud expands to a roughly 200 μm radius and falls roughly 300 μm. We demonstrate free space Ramsey spectroscopy in an ensemble of 240 000 atoms with single-shot fractional stability 3.8 dB (2.4 fold) below the QPN limit for a Ramsey time of 3.6 ms, and set the stage for spin-squeezed atom interferometry. Our reported fractional stability is limited by microwave noise in addition to the technical-limited fluorescence detection protocol.

The collective pseudospin operator in an ensemble of N atoms is the sum of the individual ones, i.e., $J_z = \sum_{i=1}^{N} \sigma_{z,i}/2 \equiv (N_\uparrow - N_\downarrow)/2$, where $\sigma_{z,i}$ is the third Pauli operator defined by the clock states $\{|\uparrow\rangle_i, |\downarrow\rangle_i\}$ of the ith atom, and $N_{\uparrow,\downarrow}$ are the number of atoms in the respective states. The coherent, or minimum uncertainty, state of an ensemble of independent atoms with the pseudospin pointing in the x direction ($\langle J_x^{\text{CSS}}\rangle = N/2$, $\langle J_y^{\text{CSS}}\rangle = \langle J_z^{\text{CSS}}\rangle = 0$) is given as the tensor product of all individual states, or $\prod_i (|\uparrow\rangle_i + |\downarrow\rangle_i)/\sqrt{2}$ where CSS stands for coherent spin state. This state has a variance of $\langle \Delta J_z^{\text{CSS}}\rangle^2 = \langle \Delta J_y^{\text{CSS}}\rangle^2 = N/4$, which is the QPN value.

Squeezing protocols redistribute the variance of J_y and J_z constrained to the relation $(\Delta J_z)(\Delta J_y) \geq |J_x/2|$. Practically, these protocols can cause a reduction in J_x. To account for both effects, the metrologically relevant squeezing is characterized by the Wineland squeezing parameter [5]

$$\xi^2 = \left(\frac{\Delta J_z}{\Delta J_z^{\text{CSS}}} \frac{N/2}{|J_x|}\right)^2. \tag{1}$$

The first ratio in Eq. (1) is the standard deviation reduction, while the second is the inverse of coherence C. As an example, $\xi = 0.51$ for the 5.8 dB squeezing recovered in this Letter.

We generate spin-squeezed atomic ensembles using an almost-homogeneous atom-probe coupling as described by Hosten et al. [9]. The QND measurement has a dual functionality: it prepares the atoms in a 14 dB squeezed state by measuring the J_z component of the ensemble spin, and it also serves as a correlation reference to the final fluorescence measurement. A 780-nm beam resonant to the optical cavity is used to probe the atoms [see Figs. 1(a) and 1(c)]. The phase shift on the back reflected light reveals the cavity resonant frequency shift which is measured using a homodyne protocol [9]. The amount of spin squeezing induced by this measurement is separately calibrated using two correlated QND measurements [18].

Fluorescence is used for population spectroscopy after the lattice is turned off and the atoms are released to free space [see Fig. 1(d)]. A 780-nm laser pulse perpendicular to
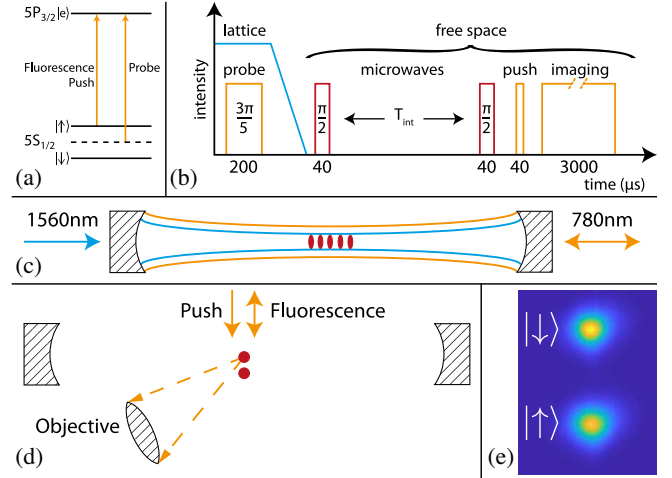

FIG. 1. Experimental procedures. (a) Relevant atomic states. The probe (QND measurement) light is tuned halfway between the $|\downarrow\rangle$ and $|\uparrow\rangle$ states whereas the fluorescence measurement is tuned directly from the $|\uparrow\rangle$ state to the $|e\rangle$ state. The probe light is on resonance with the empty optical cavity. (b) Timing sequence for the experiment. Before the steps shown here, the atoms are prepared in the presqueezed state (see Supplemental Material [19] for full sequence). The probe induces a $3\pi/5$ phase shift on the atomic spins due to the ac Stark effect. Free fall occurs between the end of the lattice ramp down and the start of the push beam. During Ramsey spectroscopy, the two microwave $\pi/2$ pulses are introduced. (c) Atoms are prepared in a horizontal cavity at the potential minima of a one-dimensional 1560 nm lattice. The 780 nm probe squeezes and measures the state. (d) After release, the cloud falls under the force of gravity. The push beam separates the states in space by giving the $|\uparrow\rangle$ state a downward momentum kick. Finally, a vertical, retroreflected, imaging beam fluoresces the atoms. Repump light (not shown) illuminates the atoms from the side during imaging. (e) A typical image for the separated clouds. The image is 5.3 mm across. The $|\uparrow\rangle$ state is pushed downward in space.

the cavity state selectively separates the atoms by applying momentum to atoms in the $|\uparrow\rangle$ state. Once the states have separated in space, fluorescence imaging is used to simultaneously count the number of atoms in each state and, therefore, estimate the J_z component of their collective spin [20]. The fluorescence detection (second measurement) returns a value of J_z within the uncertainty of the nondestructive probe (first measurement). In fact, for a given run i, the mean of the second measurement of J_z is set by the output of the first measurement, i.e., $J_{z,2}^i = J_{z,1}^i + \delta_i$, with $\langle \delta \rangle = 0$. This correlation defines the observable of interest to be the difference of the two consecutive measurements, $J_z^{(1,2)} = J_z^{(2)} - J_z^{(1)}$ [18]. Although the fluorescence population spectroscopy procedure is noisier than the QND probing, correlations between the two are preserved (see Fig. 2).

A summary of a typical experimental cycle detailed in [9] is outlined here. We generate a $\sim$25 μK gas of ^{87}Rb in an 1560-nm optical dipole lattice trap [Fig. 1(c)]. Atoms
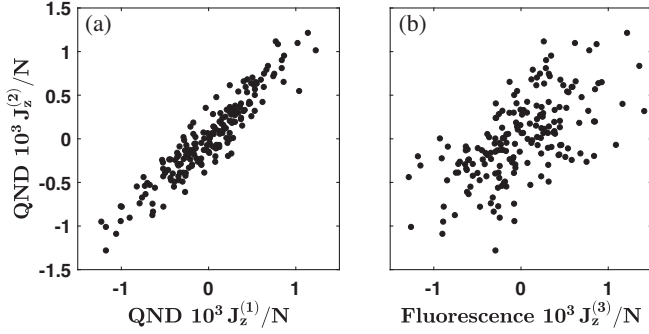
FIG. 2. Correlation between measurements of J_z/N for $N = 390\,000$. Two QND measurements, $J_z^{(1)}$ and $J_z^{(2)}$, and a fluorescence measurement, $J_z^{(3)}$, were taken sequentially. Cavity-cavity measurements (a) show a narrow linear correlation, while cavity-fluorescence measurements (b) show reduced correlations due to additional technical noise associated with fluorescence imaging.

distributed in about 1000 sites of a 1D optical lattice are prepared in a coherent 50-50 superposition of the two clock states $|\uparrow\rangle = 5^2S_{1/2}|F = 2, m_F = 0\rangle$ and $|\downarrow\rangle = 5^2S_{1/2}|F = 1, m_F = 0\rangle$ using a composite-$\pi/2$ low-noise microwave pulse (the microwave system and its phase noise performance are described in the Supplemental Material [19]). The state is then presqueezed (one-axis twisting [25]) consecutive with a 200 μs-long cavity measurement to produce the squeezing. Next, the lattice power is decreased over 0.2 ms and the atoms free fall for 4 ms before performing population spectroscopy. At this time, a laser pulse on resonance with the $|\uparrow\rangle \rightarrow |F' = 3\rangle \equiv |e\rangle$ transition is applied to the cloud from above for 37 μs to give a momentum transfer to the atoms in the $|\uparrow\rangle$ state [26]. Once sufficiently separated, a repump beam continuously pumps $|F = 1\rangle \rightarrow |F = 2\rangle$ through $|e\rangle$. A simultaneous retroreflected imaging beam 0.2 Γ red detuned from the $|F = 2\rangle \rightarrow |e\rangle$ transition induces $|e\rangle \rightarrow |F = 2\rangle$ emission in both clouds for 3 ms. Here, Γ is the atomic linewidth, $(2\pi) \times 6.06$ MHz.

The fluorescence imaging system consists of an objective lens with a numerical aperture of 0.25 and a 1:1 relay to a camera. The sensor is a commercially available low read noise CMOS camera (see Supplemental Material [19]). Each cloud is spatially well resolved on the 3.1 Mpx camera without overlap between them. Typical cloud sizes are 3 mm in diameter and remained independent of atom number. These imaging parameters are limited by the field of view of the camera and cloud expansion over time. Atom number is calibrated by measuring the cavity resonance frequency shift for atoms prepared in the ground state and correlating it with the number of detected fluorescent photons. The camera detects, on average, 65 photons per atom over the 3 ms exposure time. We correct for a slight pixel dependence on the collection efficiency.

More details of the system and these procedures are described in the Supplemental Material [19].

Rabi oscillation sequences for the CSS atomic ensemble reveal a coherence of $C \approx 0.98$ [9], squeezed-state preparation with the QND probe reduces this to $C \approx 0.91$. The coherence remains at this level after the atoms are released from the lattice. In the described configuration, the total free fall time between release and spatial state separation available to utilize the atomic spins for metrology is 4 ms due to atoms leaving the field of view of the camera. However, in an alternative configuration, by increasing the time over which the lattice power decreases to 7 ms, the cloud can be made to expand more slowly and the camera can collect images after free fall times up to 8 ms. These long free falls are possible at the cost of coherence ($C \approx 0.73$) caused by the longer exposure to the lattice potential, which results in less metrologically relevant squeezing. This expansion is our main limitation to achieving interrogation times longer than 8 ms.

Atoms preserve their coherence as well as the squeezing levels for all free-fall times explored in this Letter (Fig. 3 and Supplemental Material [19] Tab. S2). To our knowledge, this is the first demonstration of squeezing preserved in an atomic cloud that expands rapidly in space (from 17 μm rms radius to roughly 200 μm) and changes mean position (about 300 μm) between creation and detection. For the purpose of achieving the largest metrological squeezing at long times, all of the data presented below were taken using a lattice release time of 0.2 ms and a free fall time of 4 ms.

We evaluate the performance of the system to resolve small tipping angles off the equator on the spin-1/2 multiparticle Bloch sphere [Fig. 5(b)]. Measurements of such small angles are crucial for quantum state discrimination techniques and adaptive protocols for increasing atomic clock performance [27]. These angles are along the polar direction and are estimated by dividing the spin measurements by the effective radius of the sphere,
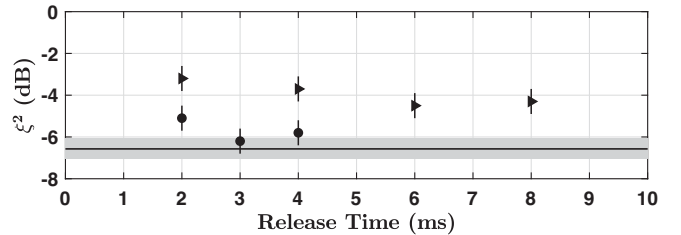

FIG. 3. Metrologically relevant squeezing ξ^2 vs free fall time for both 0.2 ms (circles) and 7.0 ms (triangles) lattice release times with $N = 390\,000$ atoms. The mean coherence of the data sets are 0.91 ± 0.06 and 0.73 ± 0.05, respectively. Values for each point can be found in the Supplemental Material [19]. Solid line: detection limit which is the same for both cases. Shaded area represents 68% confidence interval.

$\theta = J_z^{(1,2)}/C(N/2)$. All reported squeezing values are relative to a CSS with full contrast ($C = 1$).

For states near the equator, the best resolution, $\Delta\theta$, of the system is 814(61) μrad when using 390 000 atoms for a free fall time of 4 ms. These values correspond to a maximum of 5.8(0.6) dB squeezing. Even though we are able to prepare 14 dB squeezed states, the fluorescence resolved values are limited to 5.8 dB due to 740 μrad of technical noise. The largest contributions to this noise come from spin flips during the push pulse and background scattered light. A detailed description of noise sources is provided in the Supplemental Material [19]. With one-axis twisting, we prepare 7.0 dB spin squeezed state (SSS) which, when added to the technical noise, result in only 3.8 dB resolved squeezing.

Now, we utilize the squeezed states in a standard Ramsey spectroscopy sequence. 240 000 atoms are released from the lattice and rotated to a phase sensitive state by a $\pi/2$ microwave pulse about the J_x axis. After some time T_{int}, the atoms accumulate a (mean zero) phase relative to the microwave source and are then rotated back with another $\pi/2$ pulse. This pulse is phase shifted by roughly 180°. This procedure maps accumulated phase to population difference and the atoms are later state separated and imaged. In the CSS case, the atoms are prepared in the $|\downarrow\rangle$ state and two $\pi/2$ microwave pulses separated by a 90° phase shift are applied.

The performance of an atomic clock is characterized by the uncertainty of the accumulated phase, or frequency fractional stability σ_y. Assuming full contrast, the QPN limit to the stability takes the form [4]

$$\sigma_y^{(\text{CSS})} = \frac{1}{\omega_0 T_{\text{int}}} \sqrt{\frac{T_c}{N\tau}}, \qquad (2)$$

where $\omega_0 = 2\pi \times 6.834$ GHz is the atomic transition frequency, τ is the averaging time, T_{int} is the Ramsey or interrogation time, and T_c is the experimental cycle time. Our estimates of the fractional stability are limited by the noise of the fluorescence measurement, as well as noise added by the microwave source which is run independently of the atoms' dynamics.

For a Ramsey time of 3.6 ms, for example, we observe a single-shot fractional frequency stability ($\tau = T_c = 1$ s) of $8.4(0.2) \times 10^{-12}$ [Fig. 4(a)]. This corresponds to a 3.8(0.2) dB metrological improvement in performance below the QPN limit, or a 2.4 times reduction in averaging time. For $T_{\text{int}} \leq 1.3$ ms, the spectroscopy is limited by the resolution of the fluorescence imaging, corresponding to the reported 5.8 dB precision enhancement. Furthermore, we observe that the fractional stability can, in general, be averaged down while remaining below the QPN limit [Fig. 4(b)]. Microwave amplitude and phase noise, as well as magnetic field fluctuations, limit the ultimate resolution of our system to $\sigma_y \approx 4 \times 10^{-12}$.
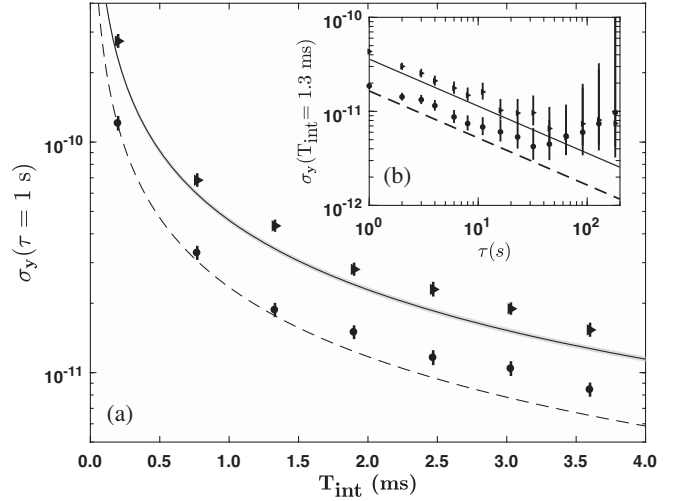

FIG. 4. Circles: squeezed state. Triangles: CSS. All error bars represent 99% confidence intervals for visual clarity. (a) Single-shot fractional stability $\sigma_y(\tau = T_c = 1$ s) for several Ramsey times T_{int} in a Ramsey spectroscopy sequence with 240 000 atoms. Solid line: QPN limit, Eq. (2). Dashed line: 5.8 dB SSS for reference. (b) Fractional stability for $T_{\text{int}} = 1.3$ ms as a function of averaging time τ.

The resolution of these types of sensors can be hindered by the inherent increase in ΔJ_y, or antisqueezing. Antisqueezing makes ΔJ_z sensitive to rotations on the Bloch sphere [28]. At large angles above the equator, the state's downward curvature projects onto J_z [Fig. 5(b)]. This issue can be tackled using adaptive measurements to
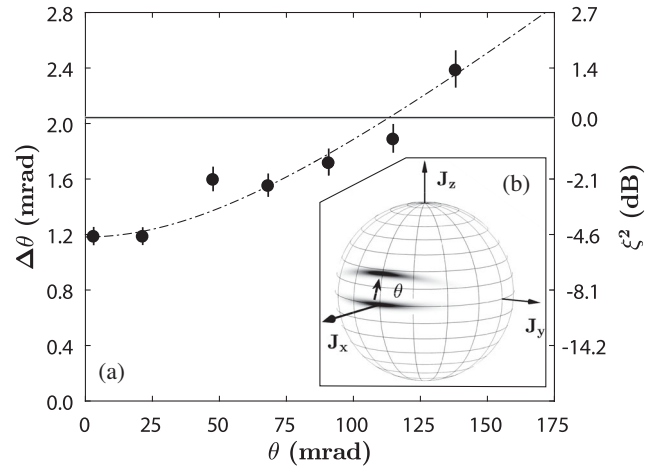

FIG. 5. (a) Angular sensitivity vs induced rotation angle for 240 000 atoms. Error bars represent 68% confidence intervals. Solid line: QPN limit, $1/\sqrt{N}$. Dashed line: theoretical fit to a squeezed state with excess antisqueezing rotated on the Bloch sphere (see Supplemental Material [19] for details). Right size scale shows metrologically relevant squeezing. (b) Bloch sphere representation of a rotated squeezed state. Figure is not to scale; the true aspect ratio of the squeezed states in the experiment is approximately 300:1.

rotate the state close to the equator before a final measurement is performed [27]. Here, we evaluate the dynamic range of our sensor; outside of which, adaptive methods would be required. We perform the above Ramsey sequence for 240 000 atoms and $T_{int} = 10\ \mu s$ with an additional phase shift of θ between the two pulses. This sequence places the state at an angle θ above the equator. The states are antisqueezed by 36 dB due to the low quantum detection efficiency of the homodyne setup [9], and the Ramsey sequence adds an extra 590 μrad of technical noise. Figure 5(a) shows the dynamic range of the measurement. Metrologically relevant squeezing can be utilized for rotations up to ± 125 mrad, exceeding by almost 2 orders of magnitude the dynamic range of the QND measurement, which is limited to angles of ± 1.6 mrad [14].

This Letter paves the way for incorporating cavity generated squeezed states into an atom interferometer. For example, a cold-atom gravimeter detects phase shifts of $\theta \propto gT^2$ where g is the local acceleration and T is the free fall time [3]. Our method would be approximately twice as sensitive as a QPN-limited sensor for the same T. Future work could include the construction of an apparatus that launches colder atoms in a fountain to increase the duty cycle.

―――――――――

[*]kasevich@stanford.edu

[1] B. J. Bloom, T. L. Nicholson, J. R. Williams, S. L. Campbell, M. Bishof, X. Zhang, W. Zhang, S. L. Bromley, and J. Ye, Nature (London) **506**, 71 (2014).

[2] R. Geiger, V. Mnoret, G. Stern, N. Zahzam, P. Cheinet, B. Battelier, A. Villing, F. Moron, M. Lours, Y. Bidel et al., Nat. Commun. **2**, 474 (2011).

[3] G. Rosi, F. Sorrentino, L. Cacciapuoti, M. Prevedelli, and G. M. Tino, Nature (London) **510**, 518 (2014).

[4] R. Wynands and S. Weyers, Metrologia **42**, S64 (2005).

[5] D. J. Wineland, J. J. Bollinger, W. M. Itano, and D. J. Heinzen, Phys. Rev. A **50**, 67 (1994).

[6] M. Kitagawa and M. Ueda, Phys. Rev. A **47**, 5138 (1993).

[7] N. J. Engelsen, R. Krishnakumar, O. Hosten, and M. A. Kasevich, Phys. Rev. Lett. **118**, 140401 (2017).

[8] L. Pezzè, A. Smerzi, M. K. Oberthaler, R. Schmied, and P. Treutlein, Rev. Mod. Phys. **90**, 035005 (2018).

[9] O. Hosten, N. J. Engelsen, R. Krishnakumar, and M. A. Kasevich, Nature (London) **529**, 505 (2016).

[10] K. C. Cox, G. P. Greve, J. M. Weiner, and J. K. Thompson, Phys. Rev. Lett. **116**, 093602 (2016).

[11] C. Gross, T. Zibold, E. Nicklas, J. Estve, and M. K. Oberthaler, Nature (London) **464**, 1165 (2010).

[12] J. G. Bohnet, B. C. Sawyer, J. W. Britton, M. L. Wall, A. M. Rey, M. Foss-Feig, and J. J. Bollinger, Science **352**, 1297 (2016).

[13] I. D. Leroux, M. H. Schleier-Smith, and V. Vuletić, Phys. Rev. Lett. **104**, 250801 (2010).

[14] Y. Wu, R. Krishnakumar, J. Martnez-Rincn, B. K. Malia, O. Hosten, and M. A. Kasevich, arXiv:1912.08334 [Phys. Rev. A (to be published)].

[15] D. B. Hume, I. Stroescu, M. Joos, W. Muessel, H. Strobel, and M. K. Oberthaler, Phys. Rev. Lett. **111**, 253001 (2013).

[16] C. D. Hamley, C. S. Gerving, T. M. Hoang, E. M. Bookjans, and M. S. Chapman, Nat. Phys. **8**, 305 (2012).

[17] We note, here, that the measurements are technically limited. Atoms are prepared with up to 14 dB of metrological squeezing using QND measurements.

[18] M. H. Schleier-Smith, I. D. Leroux, and V. Vuletić, Phys. Rev. Lett. **104**, 073604 (2010).

[19] See Supplemental Material at http://link.aps.org/supplemental/10.1103/PhysRevLett.125.043202 for additional technical details, which includes Refs. [21–24].

[20] This method is similar to the one used in Ref. [21]. However, we have improved the photon collection efficiency using a new imaging setup allowing us to perform sub-QPN measurements.

[21] O. Hosten, R. Krishnakumar, N. J. Engelsen, and M. A. Kasevich, Science **352**, 1552 (2016).

[22] E. Rocco, R. N. Palmer, T. Valenzuela, V. Boyer, A. Freise, and K. Bongs, New J. Phys. **16**, 093046 (2014).

[23] T. Pyragius, arXiv:1209.3408.

[24] R. Krishnakumar, Ph.D thesis, Stanford University, 2017.

[25] I. D. Leroux, M. H. Schleier-Smith, and V. Vuletić, Phys. Rev. Lett. **104**, 073602 (2010).

[26] G. W. Biedermann, X. Wu, L. Deslauriers, K. Takase, and M. A. Kasevich, Opt. Lett. **34**, 347 (2009).

[27] J. Borregaard and A. S. Sørensen, Phys. Rev. Lett. **111**, 090801 (2013).

[28] B. Braverman, A. Kawasaki, and V. Vuletić, New J. Phys. **20**, 103019 (2018).